Determining the Basement Fault Structure of the Hogback Monocline in Northwest NM Using Fracture Patterns and Geomechanical Modeling

Fort Lewis College

Eric Wzientek

Abstract

Monoclines on the Colorado Plateau are well understood in cross-section, but changes along strike are poorly understood. The Hogback monocline, on the Navajo Nation in northwest New Mexico, has multiple bends in map view. This study used geomechanical modeling (T7) and field data (fracture patterns) to explore the possible geometries of faults that created the bends. My research group hypothesized that under the Hogback monocline there are two possible basement fault systems a S-bend fault, two parallel faults (simple relay) These different models should show differing fracture patterns based on differing stress and strain directions.

In the field, we measured fracture sets along the monocline in the Cliff House Sandstone. We observed four sets: one parallel to the strike of bedding, two sets oblique to the strike of bedding, and one parallel to bedding dip. Fracture geometry changes as bedding orientation changes, notably around the bends. Slickenlines on some oblique fractures suggest that they are strike-slip shear fractures rather than joints.

We built two scenarios in T7 (elastic dislocation modeling, based on rock properties and structure to predict deformation). Each scenario was designed to match the geometry observed in map and cross-section view. The monocline has three bends: southern (changing strike from 014° to 057°), middle (changing from 057° to 018°), and northern (changing from 018° to 055°). Bends connecting straight segments are 2750 m long and are offset by 1650 m (northern bend) and 1900 m (southern bend). Throw on the faults was determined to be 180 m via cross sections. We tested each scenario with different boundary strain conditions and shortening directions and compared predicted fracture patterns to those observed in outcrop. Understanding timing and distribution of fractures is important for predicting the movement of oil, gas, and water, and for assessment of local subsurface risks.

Any persons wishing to conduct geological investigations on the Navajo Nation including visiting the sites described in this study must first apply for and receive a permit from the Minerals Department – Telephone (928) 871-6587.

Introduction

The Colorado Plateau is undeformed relative to the surrounding regions such as the Rocky Mountains and Basin and Range provinces. However, during the Laramide Orogeny (40-80 Ma) there was the reactivation of basement fault structures on the Colorado Plateau which created monoclines such as East Kaibab monocline, Comb Ridge, Waterpocket Fold, and the Hogback monocline (Cather, 2003). Monoclines are well understood in 2-d cross sections and when they have trend linear in map view. However, in the case of a kinked monocline the basement structure is poorly understood. The Hogback monocline in northwestern New Mexico exhibits multiple "kinked" features. To better constrain the basement structure, we looked at fractures along the anticlinal limb in the field. Later, we modeled the monocline with three proposed basement fault structures a simple relay and an S-bend fault.

The goal of the project was to determine the best fit basement structure for the Hogback monocline. In addition, we wanted determine if modeling is an effective way to predict fractures as well as create model that represents realistic geology. As part of the study, we tested different slip azimuths, to determine which slip direction could produce the fracture pattern seen in outcrop Modeling can reveal preferred stress directions, which in turn can be compared to regional tectonic concepts.

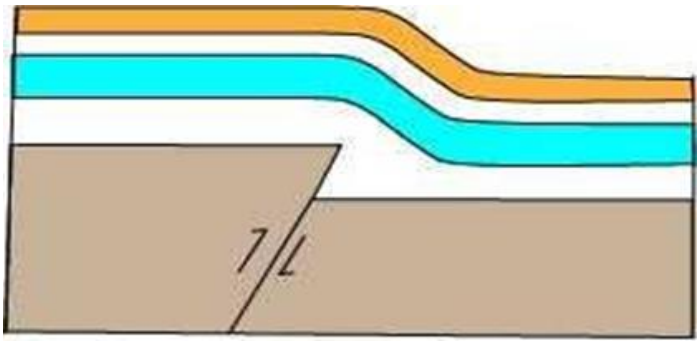

Figure 1: A cross-sectional profile of a typical monocline the most compressive force (σ 1) is left to right.

Background

Monoclines are one of the simplest and most abundant geologic structures on the Colorado Plateau. A monocline is defined as a single fold with two horizontal limbs connected by a dipping limb (Daly, 1915) (Fig. 1). Years of research and modeling have shown that regional compression and uplift are crucial in the formation of monoclines. There are two mechanisms that create monoclines. One type is called buckling, which is created by compression much like compressing a piece of paper. The other type is called forced folding, which occurs when underlying fault structures influence the folding process (Baker, 1935; Kelley, 1955; Rogers, 1987; Stern, 1992). Most, if not every, monocline on the Colorado Plateau is a forced fold. In addition, Baker (1935) and Stern (1992) interpreted monoclines to have formed above steeply dipping thrust faults, most likely in the crystalline basement.

The understanding of the mechanisms for the creation of monoclines has evolved over the years. Initially, monoclines were thought to be created by vertical forces and deep-seated vertical fractures, and compression and shortening were not considered as possible causes. Nevin (1950) suggested later that compression and shortening caused the basins, monoclines, and uplifts on the Colorado Plateau. Reches (1978) suggested that if monoclines were formed by reverse faults then the limbs would be under tension

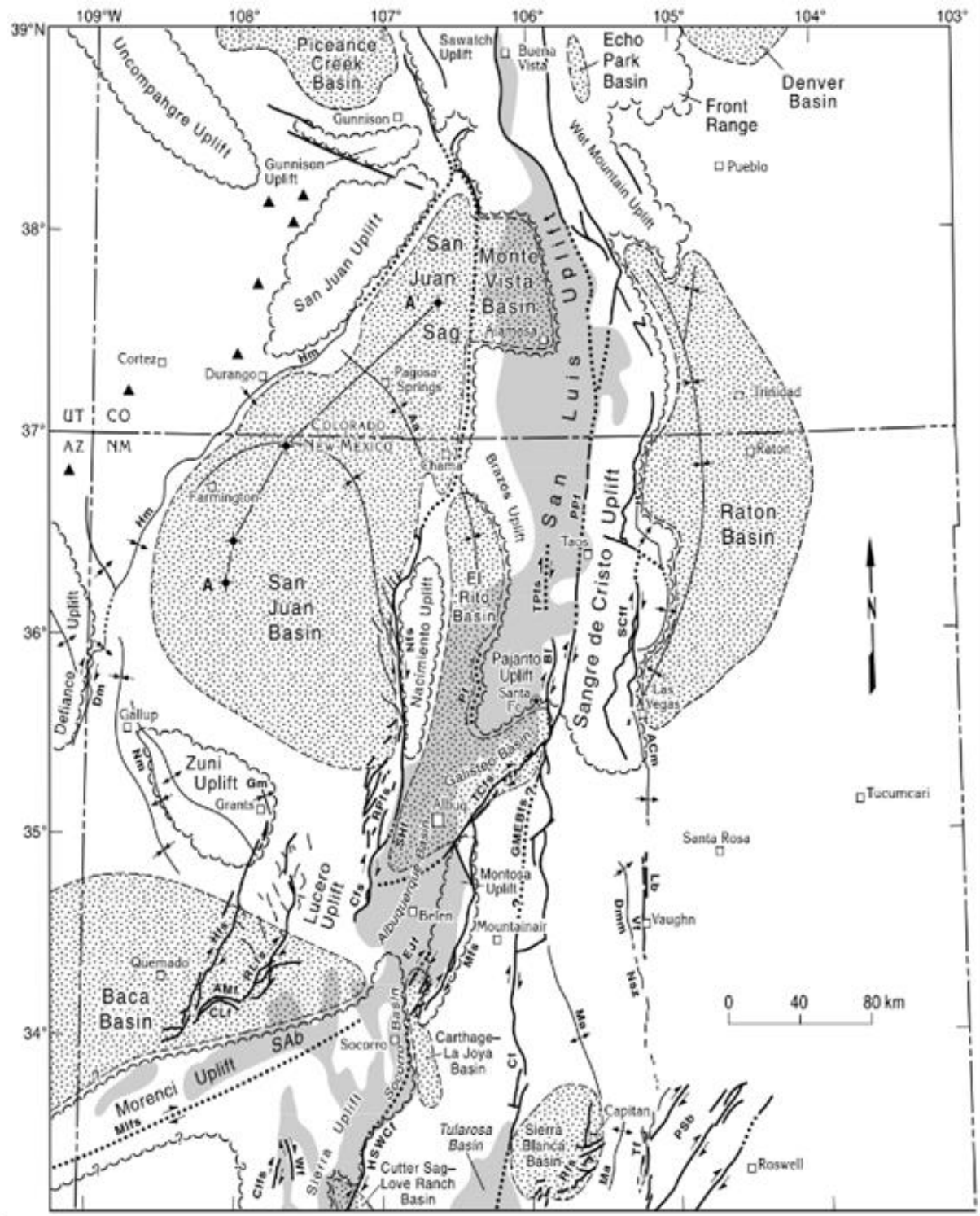

Figure 2. The schematics of the San Juan basin including the dominate structures. Note the Hogback Monocline (Hm) in northwestern, NM (Modified from Cathers 2003)

and normal faults parallel to strike will form. In contrast, if monoclines were formed by normal faults then the tension would be equally distributed.

Tectonic Inversion

Inversion tectonics is defined as a change in direction of slip on an existing fault. The basic mechanism for the reactivation of normal faults/shear zones as reverse faults is well understood (Donath, 1961; Byerlee, 1978). The probability of a fault being reactivated can be expressed by Byerlee's Law, which compares the coefficient of sliding friction and normal stress to the sum of the shear strength and cohesion of the body of rock that is not faulted (Davis and Bump, 2009).

Figure 3. A general reference map of the field area. The bedding is dipping to the southeast

Regional setting

The Mesozoic and Paleozoic strata of the Colorado Plateau overlie Precambrian rocks. During the Laramide Orogeny (80-40 Ma years ago), subduction of the Farallon plate caused compression across the Colorado Plateau, generally in an east-west direction (Coney, 1976). A number of studies have attempted to use minor structures to estimate the precise compression direction. Ziony (1966) used joint sets on Comb Ridge to interpret a Laramide minimum compressive forced (sigma 1) direction N20°E/S20°W, which is parallel to Comb Ridge (1966). In contrast, Anderson and Barnhard (1986) used fault inversion techniques along the Waterpocket fold and Teasdale monoclines to determine a maximum compressive stress direction of N65°E/S65°W.

The Laramide's orogenic timing is classified into three parts pre, syn, and post Laramide. During pre- and syn-Laramide compression there was fracturing parallel to compression and stretching in the outer arcs in fold. While in post-Laramide there was unloading perpendicular to Earth's surface (sheeting), rebound fracture perpendicular to earlier compression, and regional extension (Rio Grande) (Erslev, 2009).

Marshak et al. (2000) stated that normal faults and shear zones along the North America and more specifically Colorado Plateau have been reactivated to create the Ancestral Rockies and Laramide uplifts. He also stated that there were two dominant sets of fault orientations during the Laramide: NE and W to NW. Work in the Grand Canyon on the East Kaibab monocline showed that under monoclines in the Colorado Plateau are influenced by basement faults rather than compression alone (Cather, 2003). The

East Kaibab monocline is a perfect example of how faults influence monoclines. The East Kaibab monocline is well exposed in profile view. The Butte fault (dipping 60-70°) underlies Paleozoic and Mesozoic rocks where the west block moved up relative to the east block creating a thrust fault folding the sedimentary rocks above (Tindell, 2000). The East Kaibab monocline is not the only monocline on the Colorado Plateau that has a profile view. Allmendinger et al. (1987) demonstrated through seismic data that the San Rafael Swell shows the presence of a basement structure. In contrast, along the Hogback monocline, neither seismic data nor basement exposure allows the direct observation of the basement structure.

San Juan Basin

Basins are created because of subsidence. Subsidence is a result of a variety of causes, such as tectonic loading, thinning of the underlying crust, volcanic collapse, faulting, or excessive increases in overlaying sediment. The most common cause of basins in the southwest is faulting or extension. Normal faults create grabens and horsts. When normal faults occur, the down block is called the graben and creates a basin, and the uplifted block is referred to as the horst. The San Juan Basin is not created by normal faulting but by uplift. Uplift creates non-uniform sedimentation. The San Juan Basin has had multiple compressional uplifts: Zuni uplift to the north, Defiance uplift to the southwest, Hogback monocline to the west, Nacimiento uplift to the east, and the Archuleta anticlinorium to the northeast, shown in figure 2 (Cather, 2003). The timing of these uplifts can be determined by isopach maps which show stratigraphic thicknesses of the San Juan Basin. Differential thickening in the Lewis Shale and Cliff House Sandstone are evidence which show that the Hogback monocline is older than the Archuleta Anticlinorium (Cather, 2003).

The San Juan Basin, which sits on the east side of the Hogback monocline, had three phases of sedimentation due to the Laramide orogeny. The first phase of subsidence occurred around 74-67 Ma and can be seen in the differential thickening of the Lewis Shale in the northeastern portion of the basin (Ayers et al., 1994), followed by 6-8 Ma years of no deposition and basin widespread erosion. The second phase of sedimentation, which includes the Pictured Cliffs sandstone and the Cliff House Sandstone, occurred 67-61 Ma mostly in the northwestern region. This was again followed by another short segment of no deposition and basin wide erosion. The last phase of deposition occurred in early Eocene (Cather, 2003).

The Hogback Monocline is a NE/SW structure that borders the northwest side of the San Juan Basin in northwest NM (Fig 2). The sedimentary rocks involved in the exposed study area of the monocline are the Cliff House Sandstone and Point Lookout Sandstones (both Cretaceous), deposited in the San Juan Basin. It is thought that the extinct steeply dipping Precambrian faults got reactivated during regional east/west compression (Cather, 2003). The Hogback, unlike other monoclines, has multiple bends in map view. Some bends' trends change nearly 60 degrees within less than half a kilometer (Fig. 3). The bends are in an S shape and are at different wavelengths ranging from multiple kilometers down to half a kilometer. The best exposure and study area is outside of Waterflow, NM, where the monocline makes three distinct S-bends, all at different wavelengths.

Methods

Field Work

To fully comprehend the field area and understand the monocline, we spent multiple 8-plus-hour days in the field. The field area is lightly vegetated, which made navigating the eastern limb of the monocline manageable. In the field, we collected strike and dip data of joints and bedding. We categorized the fractures into three groups: joints paralle to the strike of bedding (strike-parallel joints, SPJ), joints oblique to strike of bedding (oblique joints, OJ), and joints parallel to dip of bedding joints (dip-parallel joints, DPJ).

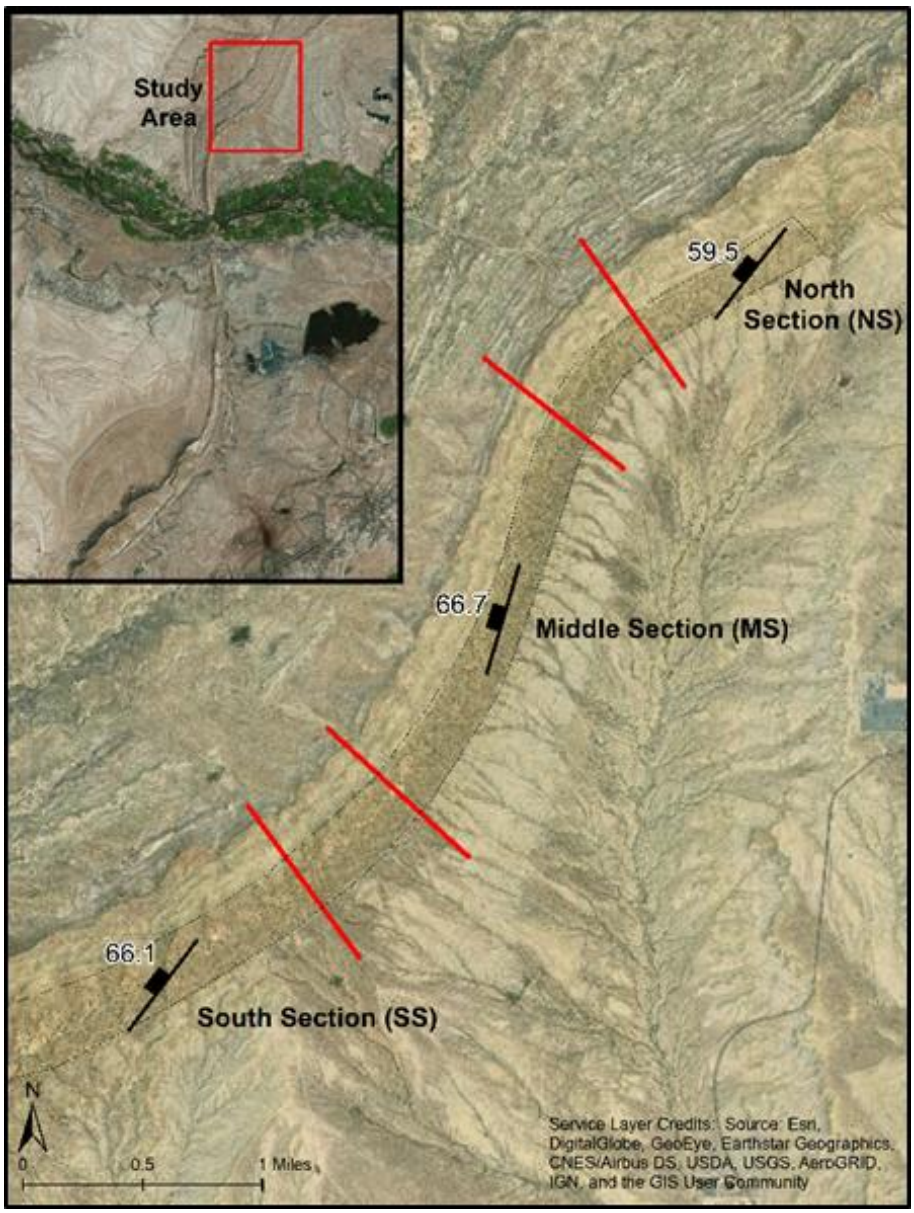

Fig 5. Map showing the separated sections. Red are boundaries between sections

To make our data more consistent we stayed on the same stratigraphic layer. This avoided differing fracture orientation due to lithologies. While collecting data, we stayed vertically staggered to make sure we didn't overlap each other's measurements. Furthermore, we wanted to get an equal amount of the four types of joints to get a good representation of the joint orientations without being biased to one or another. This means that we cannot look at the fracture intensity of each joint set along the monocline. In addition, we collected GPS coordinates for each measurement (NAD 1983 UTM Zone 13N). We also took GPS locations at places where there was high fracture intensity, mineralization in joints, S-fractures, or any unusual crosscutting relationships. On average, in a day each individual took 60-80 measurements and covered a quarter mile.

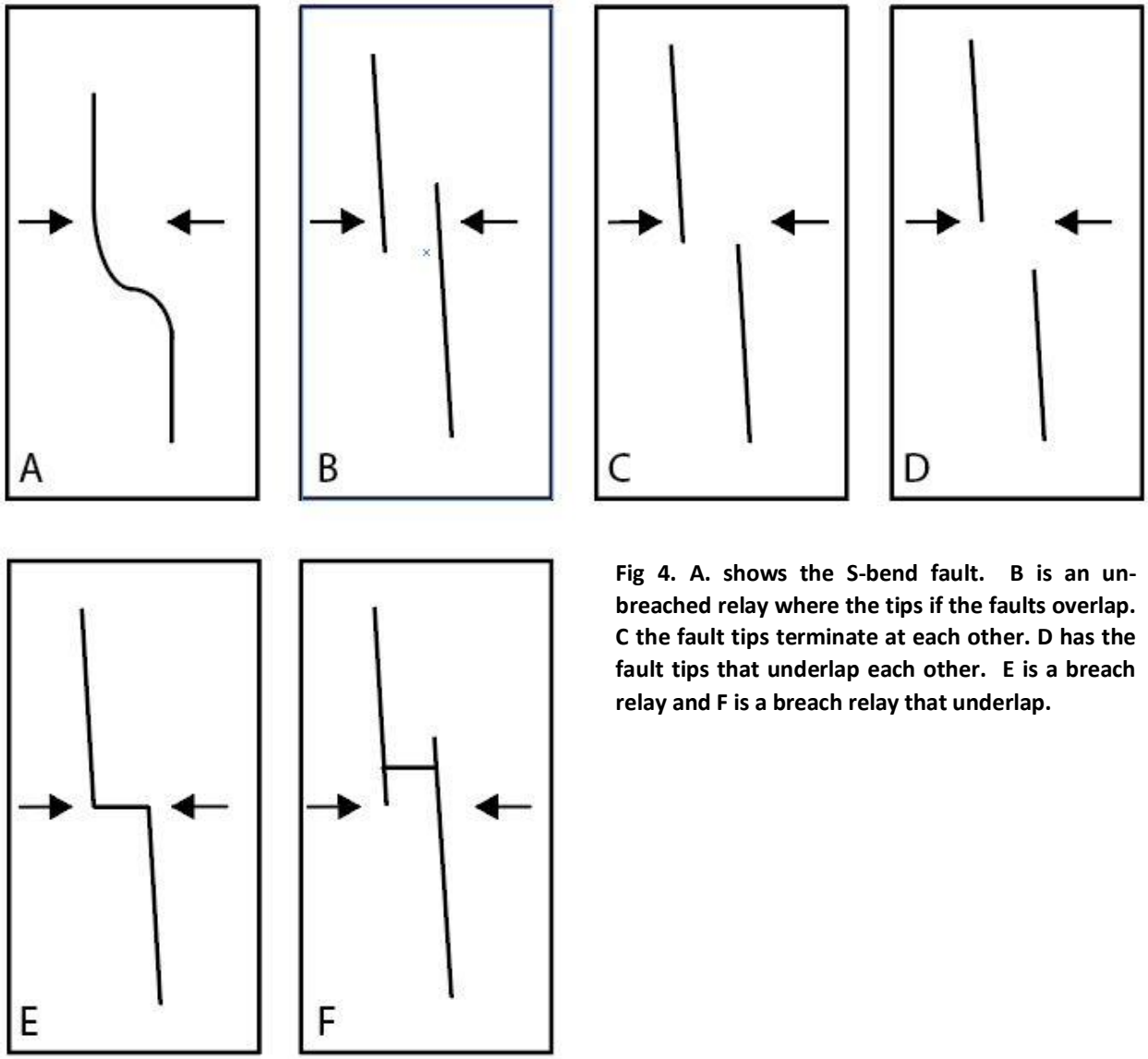

Fig 4. A. shows the S-bend fault. B is an un-breached relay where the tips if the faults overlap. C the fault tips terminate at each other. D has the fault tips that underlap each other. E is a breach relay and F is a breach relay that underlap.

On October 27, 2018 we had the Fort Lewis Geosciences Structure class assist with data collection along the specified stratigraphic layer using the same methods stated above. When the structure class took measurements, each of the 24 students took on average 25 measurement over a mile and a half area. The data when plotted in GIS was discontinuous. To correct this, we then went into the field later and collected additional data to make sure the data was continuous throughout the study area.

Once field data was imported to Excel and the fractures were sorted based on fracture type, I was able to import the data into Strabospot, which plots the GPS locations and the strike/dip on an aerial image. In Strabospot, each fracture set was separated based on the relative location on the monocline (Fig. 5). This helped produce stereonets for each segment of the monocline, such as straight sections versus the kinks.

T-Seven Modeling

T-Seven is a geomechanical modeling software which assumes an elastic rheology. This dynamic modeling predicts fracture type and orientation based on rock properties and strain parameters. The observation grid's height above the fault tip and depth below the surface were based on the exposed surface at the time of deformation via stratigraphic thickness along the San Juan Basin (Kirkham and Navarre, 2003). The displacement on the faults was determined by cross section of multiple topographic and geologic maps. Two different methods were used. First, we looked at the maximum relief from the horizontal Cliff House Sandstone. Secondly, we drew a complete cross section cutting perpendicular to the monocline. The result of these methods produced a maximum displacement of 400 to 900 meters respectively. The models calculated stress, based on elastic strain, on each of the multiple nodes which sit on the horizontal observation grid. Based on the rock strength and the local stress, the model will show tensile fractures or shear fractures. If the minimum stress (sigma 3) is below the tensile strength of the rock, the model will show a tensile fracture perpendicular to sigma 3. The orientation is based on the azimuth of stress at each node.

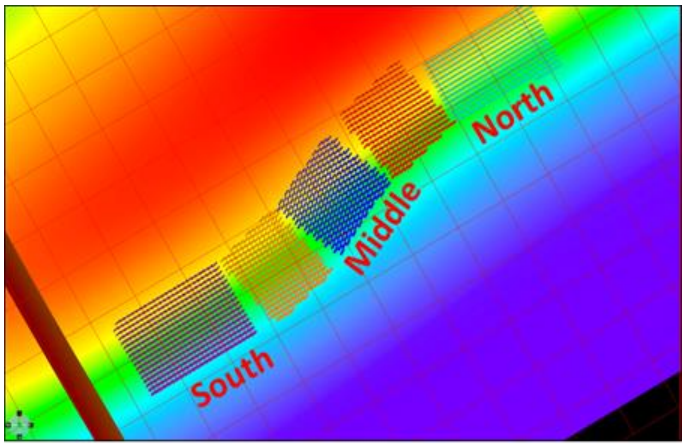

Figure 7 (above). Output from T-Seven showing differential stress from local bending of the monocline. Note the highest differential stress (red) is along the limb of the monocline.

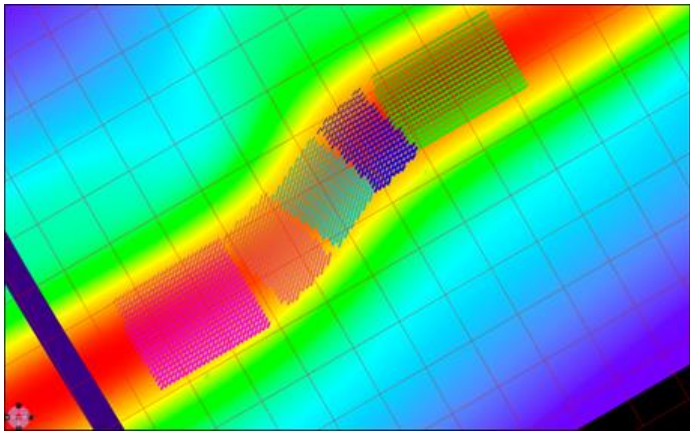

Figure 6. Elevation model of the monocline using the simple relay model at 60°. South, Middle, and North correlate to the field data's sections in figure 2.

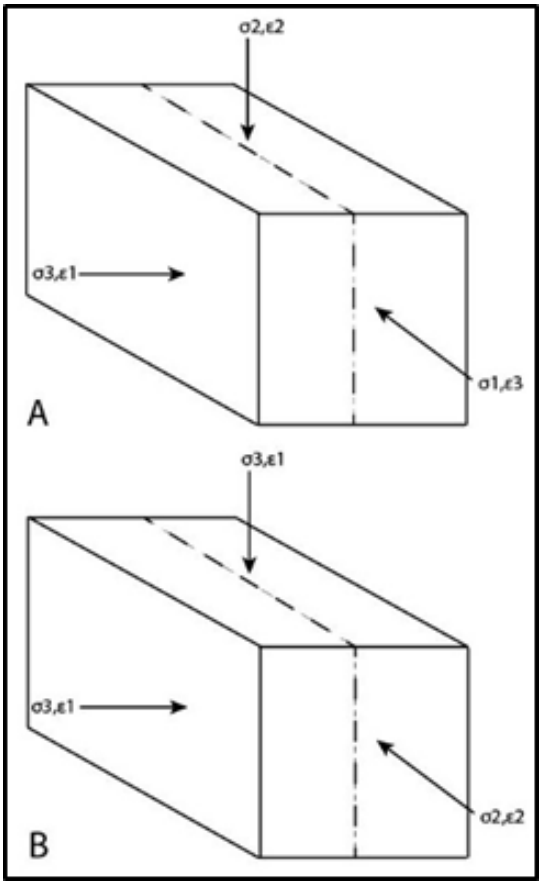

Figure 8. (left)A simple schematic showing two stress regimes to create vertical fractures. A) The option we used and is the result of a horizontal compressional environment. B) Another possible option however this forms from sediment loading

To build the 14×24×10km models in T-Seven, we first needed to know the geometry of the possible faults. The model's geometries were acquired from aerial imagery. The dip of the faults was determined by the

assumption that the basement faults are reactivated normal faults (60°-70°). Multiple models were built in T-Seven and multiple parameters were changed to find the most realistic model that visually appears the same as the field observations (Table 1). For the three hypothesized faults, we built two for each scenario with differing dips of 60° and 75°. Along with this the un-breach model had three different geometries as shown in figure 4. In addition, the breach model has two different geometries (Fig. 4). In total there are twelve separate models. The model in which this paper looked at in depth was the 60° dipping, 0 km overlapping simple relay.

Table 1. This shows the crucial parameters to which we changed in order to create the best models.

Azimuth of Stress	Strain Conditions	Throw (m)	Fault Dip
Left=300°	2.0%	400	60°
Center=330°	0.1%	900	70°
Right=360°			

With the models built the next step was to narrow down the parameters to see if we see any notable difference. One crucial step was to determine which stresses were horizontal and which were vertical. This is important because I wanted to create near vertical fractures. We used sigma 1 and sigma 3 to be horizontal and the intermediate stress to be vertical which is the case in compressive environments (Fig. 8). I changed the parameters on two different models (60° S-bend and 60° simple relay) to find the most influential parameters and to find the best parameters to use for the other ten models (Table. 2). The first parameter that was changed was making the model slip on the fault or to strain the bounds of the model by 5% and 1%. This forced the faults to slip to compensate for the strain. When running the model for having the slip be directly on the fault, we used a displacement of 900 meters and 400 meters. Furthermore, when using this parameter, I had to change the boundary constraints, or what the model will do at the boundaries. Another parameter is the azimuth of strain. This parameter is crucial when using constrained boundaries rather than having the fault slip. In addition to these parameters, I used the default rock properties for sandstone which included Poisson's ratio, rock density, cohesive strength, and coefficient of internal friction. However, the Young's Modulus was changed to 20,000 mega-Pascals which represents most sandstones.

Once the parameters were changed, I was able to visually inspect the outcome to see if A) geometries compare to that of the Hogback monocline such as wavelength, relief, and if it created a bend and B) whether the orientation and type of fractures matched those observed on the Hogback monocline. To help further identify each model an added vertical observation grid, along with the horizontal horizon, was added to determine if fractures make sense at depth.

Model Output

We ran the new parameters on two models, the 60° S-bend and the 60° simple relay. Once the models were finished, they were qualitatively inspected to see if they compared to our field observations. To do this I looked at the general shape of the monocline this included wavelength, elevation displacement (Fig. 6), fracture orientation and dip, as well as if the model created a bend. To grasp the data quantitatively I created fracture networks, and looked at sigma 3 and differential stress (Fig. 7). The fracture network allowed the fractures to be exported out of T7 and into a stereonet program. In T7, fractures were exported together based on their relative location on the monocline similar to the method used for grouping the field data in Strabospot.

Table 2. Showing the average strike of SPJ fractures for the north and south section with different slip azimuths.

	Slip Azimuth		
Section	Left	Center	Right
North	072.5°	059.3°	041.5°
South	071.1°	049.0°	030.5°

Results

Field Observations

A first look at the monocline shows the segments change strike and are connected by multiple bends (Fig. 5) Three fracture sets were observed in the field: one parallel to the strike of bedding (SPJ), three sets oblique to the strike of bedding (OJ), and one parallel to bedding dip (DPJ) along with bedding. The fracture sets all changed strike along the monocline (Fig. 9). In addition, their intensity varied spatially, and cross cutting relationships changed from north to south along the monocline. Aperture of joints varied from 0.5 mm to 0.5 m. Some fractures, most notably

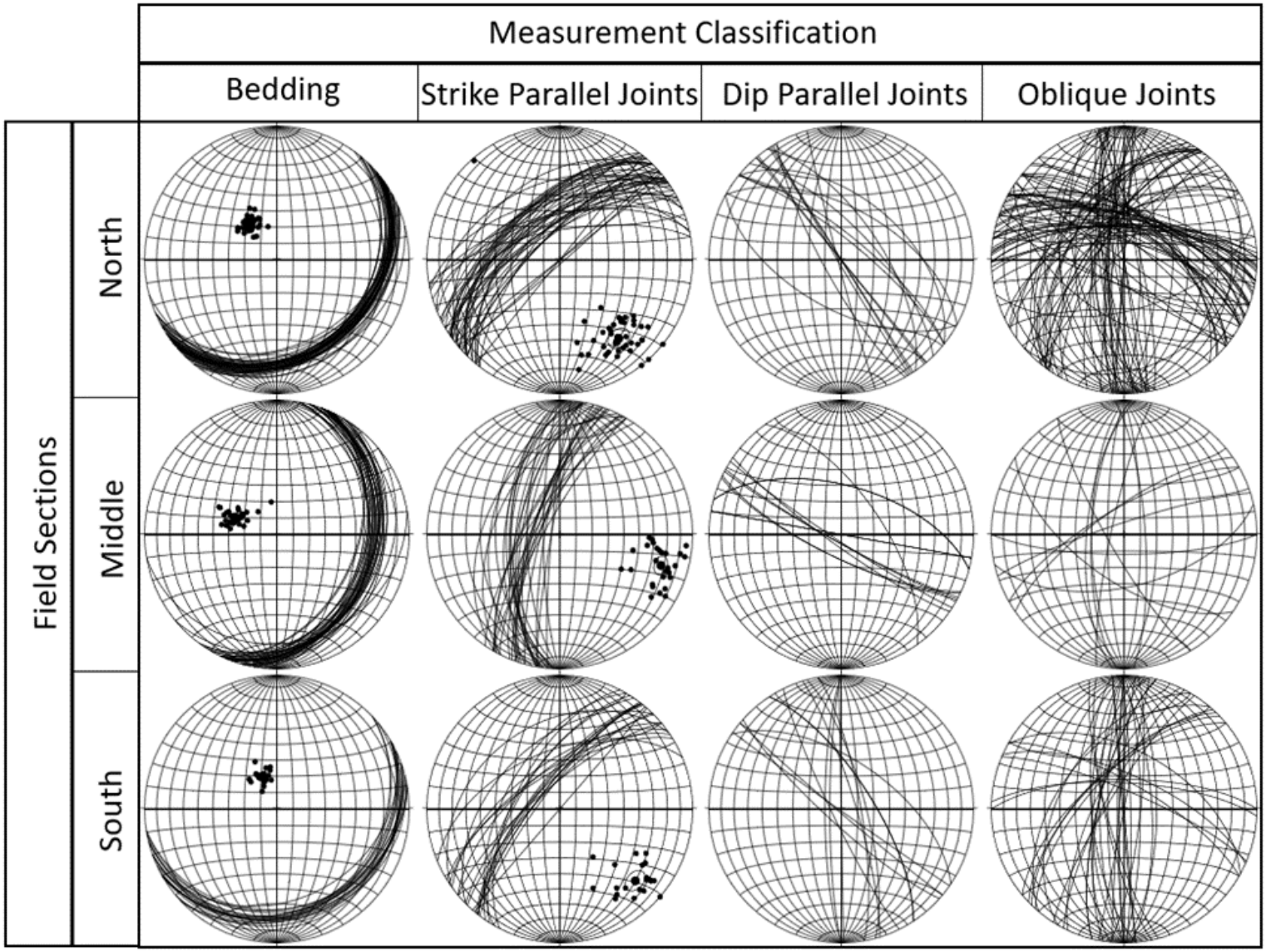

Figure 9. This shows the field data's stereonets. The field sections correlate to the reference map (Fig. 3). The bedding changes strike similar to the trend on the monocline. The SPJ fractures are striking NE/SE. The DPJ fractures are 90° from SPJ at NW/SE. The OB fractures have three distinct sets: N/S, WNW/ESE, and NNE/SSW.

in one set of OJ fractures, had mineralization and deformation bands. Along with mineralization we saw evidence of slickenlines, again on a set of OJ fractures. However, because of extensive weathering the sense of shear was not able to be observed. Some of the slickenlines were bed-parallel striations.

T-Seven

All of the computed models produced an obvious bend and near-vertical fractures. All models only produced SPJ fractures rather than the other fracture sets. This is because T-Seven shows the first fracture that forms given the stress reached at each individual grid node. A lower strain of <0.5% created vertical fractures while higher strain produced fractures with gentler dips. The azimuth of strain of 300°(right) was better than 360°(left). However 330°(center) created the most noticeable change in SPJ fracture orientation (Table 2). When the model ran based on forcing the fault to move, we saw more vertical

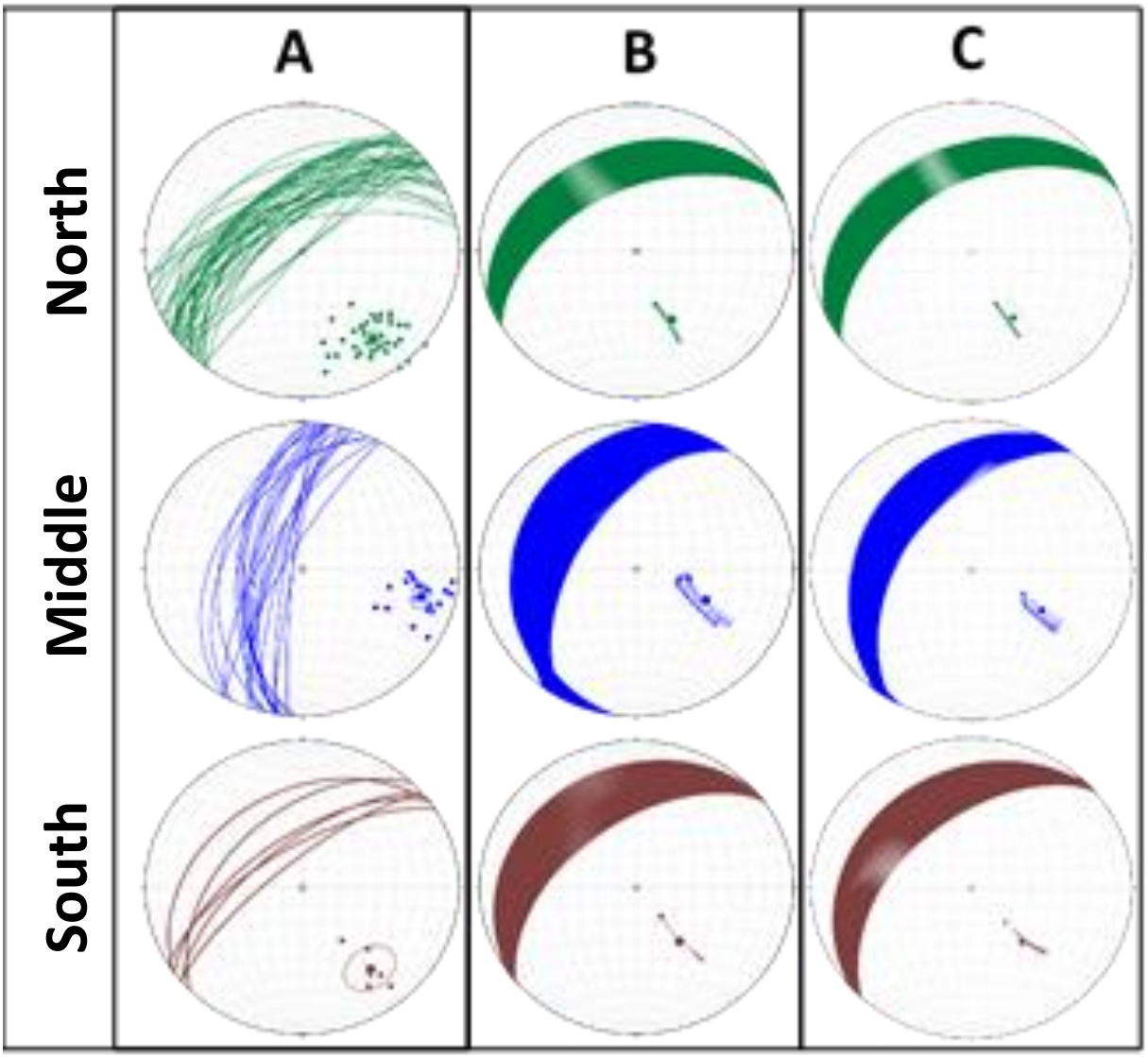

Figure 10. (A) Field data strike averages are North (NS): 053°, Middle (MS): 013°, South (SS): 052°. The difference between NS-SS and the MS is 39.5°. (B) the S-Bend fault's models strike averages are NS: 065°, MS: 025°, and SS: 054°. The difference between NS-SS and MS is 34.5°. (C) the simple relay model's strike averages are NS: 059°, MS: 031°, and SS: 049°. The difference is 23°.

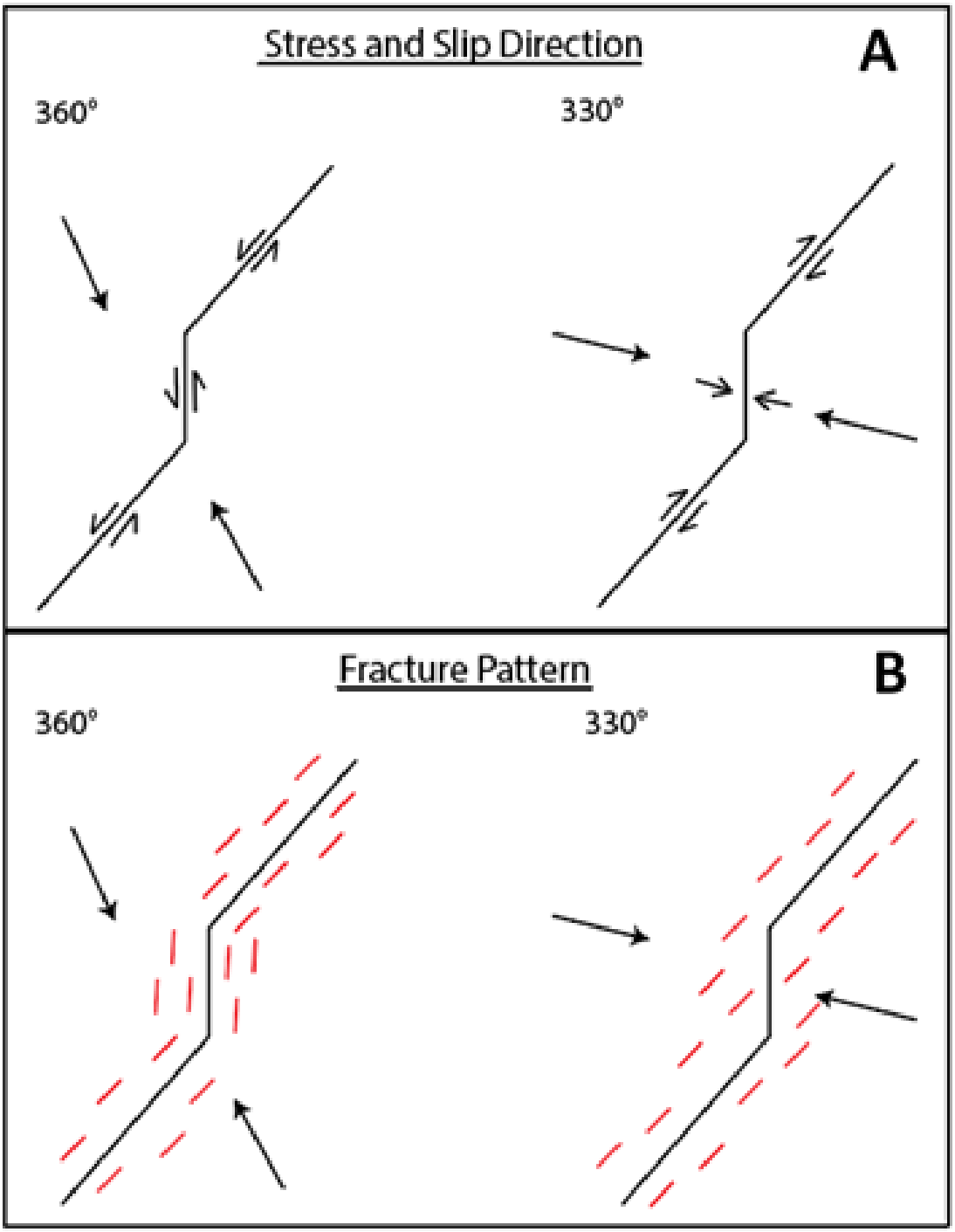

Figure 11. A) shows the regional stress parameters B) is the fracture prediction based on the slip

fracture. This contrasted with the other option of compressing the boundaries and letting the faults compensate for the strain. The 60° S-bend and 60° Simple Relay fault models' fracture outputs show a change in strike most noticeably on the middle section and north/south sections (Fig. 10).

Discussion

The three sets of fractures observed in the field are DPJ, SPJ, and OJ on the anticlinal limb of the monocline. The DPJ fractures have a general strike of NW/SE. The SPJ fractures strike NE/SW. The OBJ fractures have three distinct subsets: One which strikes N/S, another which strikes NW/SE, and one which strikes NE/SW. The NE/SW set of OBJ fracture had slickenlines, which suggest they are shear rather than tensile which characterize the other fracture seen in the field. Because of cross cutting relationships and mineralization along the N/S OJ fractures we can determine the relative timing of fractures. The N/S OB fractures, which were mineralized, occurred the earliest. Other fractures changed crosscutting relations along the monocline.

Fault Models

The two models had different basement fault structures simple relay and a S-bend fault. The two hypothesized models have different fault structures, but the segment length, strike, and dip were held constant between them. Some models generated SPJ fractures in which the strike didn't change throughout the longitudinal profile of the monocline. In contrast, some models produced SPJ fractures that changed strike; these changes were often subtle but still noticeable (Fig.10). All three of the hypothesized models created a bend in map view in T7. However, certain parameters created fracture patterns which better matched what we observed in the field. The parameters on the three fault models were dependent on boundary stress and stress/fault slip azimuths. The models of choice were ones in which the greatest differential stress and smaller sigma 3 along the monocline. This is because we expect tensile fracture to occur where sigma 3 is the greatest.

SPJ Fractures

With the model's stress directions, based on literature, the model should have produced OJ and DPJ, unless different stress regimes and stress azimuths changed as the formation of the monocline progressed. In contrast, we saw (1) tensile fractures at the depth of interest and (2) SPJ along the monocline. We certainly had models with other fracture types and orientations. This is because the SPJ fractures correlates to a local elastic stress regime (such as bending a sheet), rather than a regional stress regime. The SPJ fractures' strikes change along each section of the monocline (first straight, first bend, etc). This is to be expected because the monocline changes trend. When the rocks start to bend, we see extension along the anticlinal limb of the monocline. If the synclinal limb was exposed, there might not be SPJ fractures The SPJ fractures in the model most notably change strike when the slip azimuth is 30° to the right (360°) of 330° which is perpendicular to the fault (Fig 11B). While looking at the geometry of the bend this is accurate and to be expected. Fractures were collected along the center of the monocline in the field likewise in the model because the edges get affected by boundary strain conditions. This explains

why the left models are better than the right models. However, a slip azimuth of 300° created a better fracture geometry than the slip azimuth of 330°.

Vertical Plane

The vertical observation planes looked comparable for all models (Fig. 12). Field observations have shown very few shear fractures. However, in the Lewis Shale, which is stratigraphically lower that the Cliff House, we saw more evidence of shear. These observations correlate to most of the models, where the Cliff House is expressing all tensional fractures. This could be due to the difference in burial depth and or different rock properties between the shale and the sandstone.

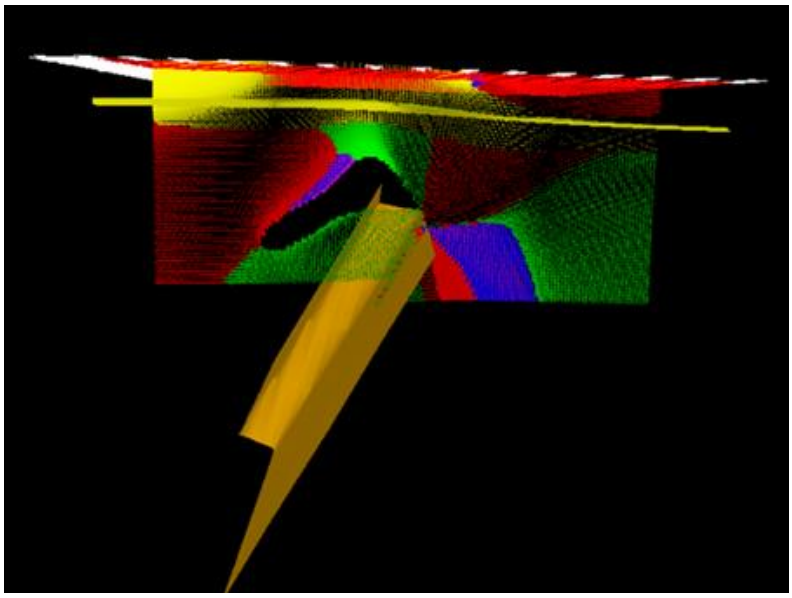

Figure 12. Cross-sectional view of a T-Seven model. Fracture types: Yellow-tensile, Red-normal shear, Green-reverse shear, Purple- oblique shear

Regional Stress

Regional stress along the monocline took place during two separate times. Stress parallel to the DPJ fractures can determine the regional stress at one time. The range of that stress along the monocline is N40-70W°/ S40-70E°. This contrasts with Anderson and Barnhard (1986)'s findings of a maximum compressive stress direction of N65°E/S65°W along the Waterpocket fold. However, our stress direction for the DPJ fractures correlate well with Davis (1999), whose conclusion of the San Rafael Swell produced a maximum stress direction of N60W°/ S60E°. and Ziony's (1966) conclusions of a stress direction of N70W°/ S70E° for the Monument uplift. Our DPJ fracture data is also consistent with the Kaibab uplift, N55W°/ S55E° Reches (1978), Davis (1999), and Tindall and Davis (1998). The SPJ fractures were NE/SW, which correlate to Anderson and Barnhard (1986).

Conclusion

Four sets of fractures are found on the Hogback monocline: dip-parallel joints (DPJ), strike-parallel joints (SPJ), and three sets of oblique joints (OBJ). The dip parallel was the least common in the field area and ranged in strike along the monocline from N40-70W°/ S40-70E°. One set of OBJ striking N/S which were heavily mineralized and had some evidence of shear. The other two set of OBJ fractures strike WNW/ESE and NNE/SSW (Fig. 9). OJ fractures were the most common type of fracture in the field area. SPJ fractures strike N25-60W°/ S25-60E°. SPJ fractures changed strike as the monocline trend changes.

All 12 models produced both a change in elevation (a monocline) and a bend in the monocline. In addition, the modeling predicted the formation of tensile fractures that were similar in orientation to the strike-parallel joints. We determined the best parameters to be <1% strain and most importantly a slip azimuth of 330°. When all the models were running under the same parameters, we found the model data was

similar to that of the field data, and what changed the strike was the azimuth of slip rather than the basement structure.

SPJ fractures were the most important sets in this study because they were compared to that of the models. The model did not produce DPJ fractures and OJ fractures, which are used more in looking at the regional stress. In contrast, the model only produced SPJ fractures because of the localized elastic stress due to the bending of the monocline. The maximum stress direction of the DPJ/OJ fracture correlate to the NW/SE and NE/SE stress directions of the Laramide (Davis and Bump, 2003).

Modeling was an effective technique to predict fractures. The modeling software expected elastic deformation which created fractures along the strike of the monocline. Future work would involve taking more measurements along the southern portion of the monocline. In addition, testing more parameters such as rock properties, different strain azimuth, different horizon depths, and different depth of the fault tip. Furthermore, more research needs to be done looking at fracture density and analog modeling. Analog modeling would recreate a scaled-down version of the digital models. Comparing analog modeling, geomechanical modeling, and field work would be crucial in further research as it has not been done before.

References

Allmendinger, R., Hauge, T., Hauser, E., Potter, C., Klemperer, S., Nel-son, K., Kneupfer, P., and Oliver, J., 1987, Overview of the COCORP 40°N transect, western United States: The fabric of an orogenic belt: Geological Society of America Bulletin, v. 98, p. 308–319, doi: 10.1130/0016-7606(1987)98<308:OOTCNT>2.0.CO;2.

Ayers, W. B., Jr., and Kaiser, W. R., 1994, Coalbed methane in the Upper Cretaceous Fruitland Formation, San Juan Basin, New Mexico and Colorado: New Mexico Bureau of Mines and Mineral Resources, Bulletin 146, 216 p.

Baker, A. A., 1935, Geologic structure of south-eastern Utah: American Association of Petroleum Geologists Bulletin, v. 19, p. 1472-1507.

Bump, A., and Davis, G.H., 2002, Forward and inverse trishear modeling of the San Rafael and Waterpocket monoclines, Colorado Plateau, Utah: Geological Society of America Abstracts with Programs, v. 34, no. 6, p. 4.

Coney, P.J., 1976, Plate tectonics and the Laramide orogeny: New Mexico Geological Society Special Publication 6 – Tectonics and mineral resources of southwestern North America, p. 5-10.

Cather, M. S., 2003, Polyphase Laramide tectonism and sedimentation in the San Juan Basin, New Mexio: New Mexico Geological Society 54th Annual Fall Field Conference, p. 119-132.

Davis, G.H., 1999, Structural Geology of the Colorado Plateau Region of Southern Utah, with Special Emphasis on Deformation Band Shear Zones: Geological Society of America Special Paper 342, 157 p.

Daly, R. A., 1915, A geological reconnaissance between Golden and Kamloops, B. C., along the Canadian Pacific Railway: Geological Survey of Canada Memoir 68, 260 p.

Marshak, S., Karlstrom, K., and Timmons, J.M., 2000, Inversion of Proterozoic extensional faults: An explanation for the pattern of Laramide and Ances-tral Rockies intracratonic deformation: Geology, v. 28, p. 735–738, doi: 10.1130/0091-7613(2000)28<735:IOPEFA>2.0.CO;2.

Nevin, C. M., 1950, Principles of Structural Geology: New York, Wiley, 410 p.

Rodgers, J., 1987, Chains of basement uplifts within cratons marginal to orogenic belts: American Journal of Science, v. 287, p. 661–692.

Reches, Z., 1978, Development of monoclines: Part 1. Structure of the Palisades Creek branch of the East Kaibab monocline, Grand Canyon, Arizona: Geological Society of America Memoir v. 151, p. 235–272.

Stern, Sharon, 1992, Geometry of basement faults underlying the northern extent of the East Kaibab monocline, Utah: Chapel Hill, University of North Carolina, M.S. thesis.

Tindall, S. E., 2000, The cockscomb segment of the East Kiabab monocline: 2000 Utah Geological Association Publication 28

Tindall, S.E., and Davis, G.H., 1998, Partitioning of faulting within a reverse, right-lateral shear zone along the East Kaibab monocline, Colorado Plateau, Utah: Geological Society of America Abstracts with Programs, v. 30, no. 6, p. 38.

Windley, B.F., 1995, The Evolving Continents: Chinchester, John Wiley and Sons, 526 p.

Ziony, J.I., 1966, Analysis of Systematic Jointing in Part of the Monument Upwarp, Southeastern Utah [Ph.D. thesis]: Los Angeles, University of California, 112 p.